Scientific Research Publishing

Smart Grid and Renewable Energy, 2026, 17(11), 390-414
https://www.scirp.org/journal/sgre
ISSN Online: 2151-4844
ISSN Print: 2151-481X

Estimation of Wind Energy Potential Applied to Water Pumping in the Bodélé Triangle Area (Tibesti-Ennedi-Lake) in Chad

Fia Oung-Zetna[1,2*], Zoutchibé Joseph[2], Gotoum Nadjinangar[2], Laleko Benjamin[2], Foulla Dieudonné Platou[2], Noel Djongyang[1]

[1]Department of Physics, University of Maroua, Maroua, Cameroon
[2]Department of Physics, University of N'Djamena, N'Djamena, Chad
Email: *fiaoungzetna@gmail.com

How to cite this paper: Oung-Zetna, F., Joseph, Z., Nadjinangar, G., Benjamin, L., Platou, F.D. and Djongyang, N. (2026) Estimation of Wind Energy Potential Applied to Water Pumping in the Bodélé Triangle Area (Tibesti-Ennedi-Lake) in Chad. *Smart Grid and Renewable Energy*, **17**, 390-414.
https://doi.org/10.4236/sgre.2026.1711018

Received: August 14, 2026
Accepted: November 24, 2026
Published: November 27, 2026

Copyright © 2026 by author(s) and Scientific Research Publishing Inc.
This work is licensed under the Creative Commons Attribution International License (CC BY 4.0).
http://creativecommons.org/licenses/by/4.0/

Open Access

Abstract

The use of renewable energies, such as wind and solar energy, is an important solution to deal with climate change in Chad. Renewable energy sources are not only more environmentally friendly, but they are also more sustainable and less expensive in the long run. With regard to water pumping, the use of wind energy can help reduce dependence on fossil fuels. In northern Chad, where climatic conditions are arid and rainfall is rare, the assessment of wind pumping potential can be a viable solution to provide water for the population, livestock and irrigation. In this zone, the wind speed exceeds 4 m/s and reaches 9 m/s at the height of the aerogenerators. It can be seen that the hourly values are higher than the monthly and annual values of the wind speed. We have chosen for the three wind turbines AN Bonus 1 MW, HSW 1000/57 and Vestas 2 MW/40 for the pumping. The average value of the capacity factor is greater than 0.35. The electrical power varies between 357.97 kW/m^2 to 622.90 kW/m^2 for the town of Bol; 600.97 kW/m^2 to 901.24 kW/m^2 for Faya Largeau and 519.38 kW/m^2 to 751.89 kW/m^2 for Ounianga Kebir. The daily flow for the three wind turbines and the three sites varies between 48,916 m^3/day to 157,690 m^3/day.

Keywords

Bodélé Triangle, Weibull Distribution, Rayleigh Distribution, Power Density, Power Factor, Daily Flow Rate

1. Introduction

Water is the vital source for all living beings on planet Earth. The absence of water

in a natural environment reflects the absence of life in it [1]. The available natural water reserves are made up of groundwater (infiltration, groundwater), stagnant surface water (lakes, dam reservoirs) or flowing (rivers) and seawater [2]. Many people on earth experience water scarcity and struggle daily to find clean water to meet their basic needs. Water-related natural disasters, such as floods, tropical storms and tidal waves, cause heavy loss of life and great suffering [3] [4]. Too often, drought strikes some of the world's poorest countries, worsening hunger and malnutrition [5] [6]. Over the past decade, significant progress has been made in providing people with safe drinking water and adequate sanitation services [7]. But much remains to be done over the next decade to provide these essential services to those who still lack them, the vast majority of whom live in poverty.

Wind energy is produced by the force of the wind, which turns wind turbines (or aerogenerator) for the production of electricity. It is a renewable energy source because it uses an inexhaustible natural resource, which is the wind [8]. Wind energy is growing worldwide to meet energy needs while reducing greenhouse gas emissions in strict respect for the environment.

Chad is a vast territory of sub-Saharan Africa covering an area of 1,284,000 km^2, of which 60% of the territory is desert. Its geographical location makes it the country that is bearing the brunt of the effects of climate change [6] [9]. This is reflected in the accentuation of recurrent droughts and floods; the reduction of agricultural land; environmental and soil degradation; the continuous drying up of rivers and Lake Chad; the decrease in fish, wildlife and fodder resources; the rural exodus from the northern zone to the southern zone and the intensification of conflicts between farmers and herders [10]. Faced with these multiple problems that threaten the lives of the population, the problem of water pumping is acute in Chad and constitutes a major challenge for most people who live in extreme poverty.

In this vast desert of the country, a natural phenomenon is taking place capable of generating violent winds. The Bodélé depression, located in the northern part of Chad, with a surface area of 22,000 km^2, or 0.25% of the surface area of the Sahara, is considered the dustiest place on the planet [11] [12]. The triangular-shaped zone between the Tibesti and Ennedi massifs and the lake is unique in the world, the most subject to the action of very violent winds during a good period of the year, seven months a year, after CAPOT-REY in 1961 [13]. Moreover, between the series of escarpments, these violent winds of the trade winds, which sweep the sandstone plateaus of the North-East, lead to the formation of long dune cords which separate or border the lakes [14]. These wind forces imprint specific structures on the reliefs or give them spectacular shapes.

It has been shown that the Bodélé area located in northern Chad is the only place in the world that has all the conditions to generate strong winds. According to a study conducted by a group of NASA researchers and other researchers, the wind from this part of the Sahara desert carries 182 million tons of dust to the Amazon every year over a distance of 5000 kilometers [15] [16]. This wind of sand

from the desert, carrying dust over thousands of kilometers, can be a source of energy to serve the population of this arid, bare, and desolate zone in the shape of a triangle. The purpose of this article is to assess the wind energy potential of the main cities of this Bodélé triangle.

2. Study Area and Wind Data

The macro-regional study area is geographically defined by the triangle bounded by the localities of Bol (South), Faya-Largeau (North), and Ounianga-Kébir (North-East), as illustrated in Figure 1. These three meteorological stations were selected as peripheral boundary vertices to frame the regional atmospheric and climatic gradient across the northern-central Chadian basin. A clear distinction is made between this macro-regional pre-selection phase—aimed at screening the overall spatial wind potential across the enclosed zone—and the localized micro-scale evaluation focused strictly on the Bodélé depression itself, where site-specific wind energy and water pumping dynamics occur.

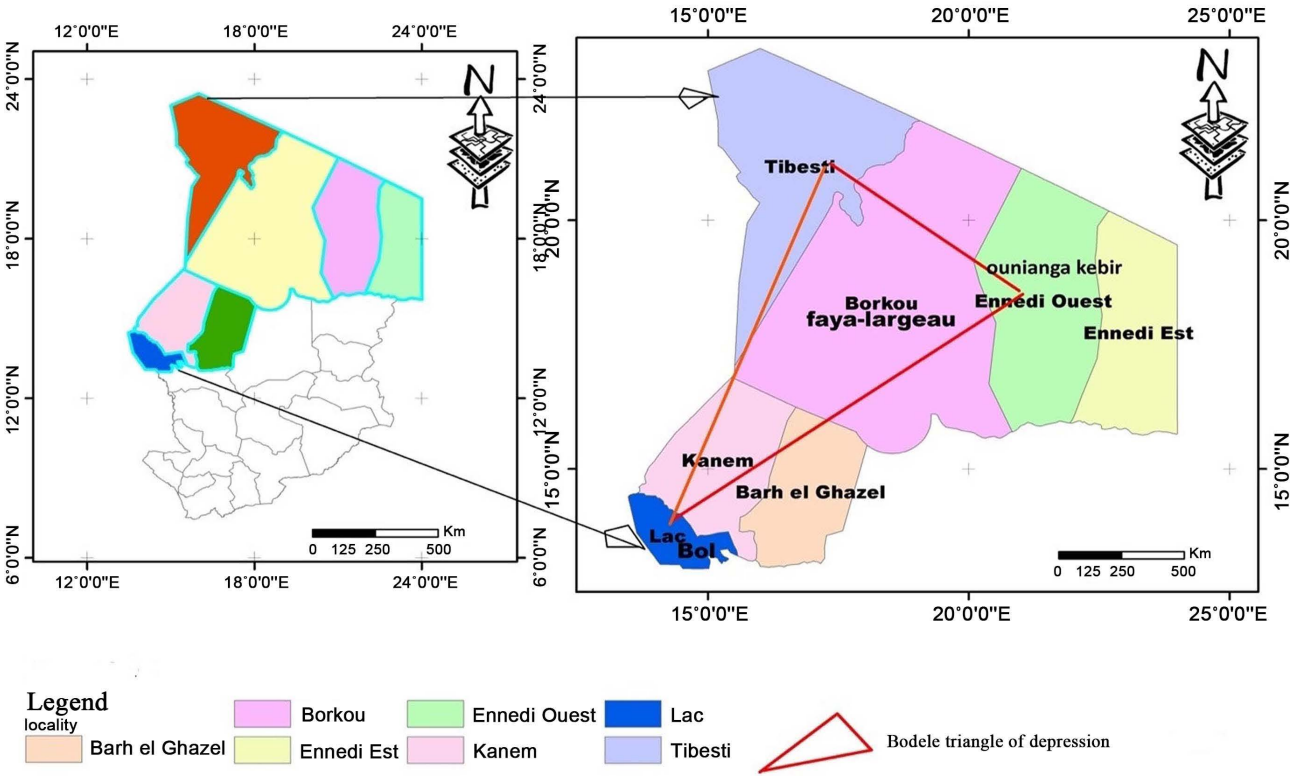

Figure 1. Map of the study area.

All meteorological data for this study were retrieved exclusively from the NASA POWER database covering the 20-year period from 2000 to 2020 in Table 1. Data extraction was conducted point-by-point using the precise geographical coordinates of the three boundary stations (Bol, Faya-Largeau, and Ounianga-Kébir). The analyzed parameters include mean wind speed as well as high-resolution maximum speed, both recorded at the standard reference height of 10 meters

above ground level (AGL). The dataset also incorporates hourly observations of wind speed and direction at this same height.

Data quality control of the hourly time series involved identifying and filtering out outliers caused by assimilation artifacts. Minor data gaps were imputed using hourly linear interpolation. To ensure consistency across parameters, mean and maximum wind speeds were aggregated to daily time steps and standardized using the z-score method to guarantee spatiotemporal coherence among the extracted datasets.

Table 1. Geographical coordinates of the study area.

Cities	Latitude	Longitude	Altitude (m)
Bol	13˚45	14˚71	293.33
Faya Largeau	17˚92	19˚12	337.57
Ounianga Kebir	19˚05	20˚49	464.6

3. Material and Methods

3.1. Material

This article aimed at the energy potential of the Bodélé depression zone. For this, we used the materials for data collection and analysis. The data were collected on the NASA website and from the National Meteorological Department of Chad. We used MATLAB R2020, Excel, Arcgis and WRPLOT software for data analysis and processing.

3.2. Mathematical Models of Wind Speed Distribution

To better assess the wind energy potential of a site, it is important to express the frequency distribution of the wind speed. Modeling studies of the wind speed distribution are oriented towards models combining power and exponential [1] [17].

These different statistical models are as follows: The Weibull distribution, the hybrid Weibull distribution, and the Rayleigh distribution.

3.2.1. Weibull Distribution

Its exponential function with two parameters makes it possible to characterize the frequency distribution of wind speeds over a given period [18] [19]. It includes a scale parameter C (m/s) which provides information on the average wind speed characteristic of the site and a shape parameter k (dimensionless) indicating the more or less pointed character of the distribution. The probability density function takes the form [20]:

$$fw(v)=\left(\frac{k}{c}\right)\left(\frac{v}{c}\right)^{k-1}\exp\left(-\left(\frac{v}{c}\right)^{k}\right) \quad (1)$$

The corresponding Weibull cumulative distribution function $F(V)$ is:

$$F(v)=1-\exp\left(-\left(\frac{v}{c}\right)^{k}\right) \tag{2}$$

This expression reflects the probability density where the wind speed remains above the average value. This function is more commonly used in the case where the wind frequency is greater than 15% [21] [22].

3.2.2. Rayleigh Statistical Distribution

The Rayleigh distribution function is the oldest empirical formula. This function is a special case of the Weibull distribution for $k=2$ is given by [23] [24]:

$$f(v)=2\frac{v}{c^{2}}\exp\left(-\left(\frac{v}{c}\right)^{2}\right) \tag{3}$$

3.3. Determination of Weibull Parameters

Standard Deviation Method

This method allows us to determine the parameters k and c from the average speed and the standard deviation by the following relations [25] [26]:

$$k=\left(\frac{\sigma}{\overline{v}}\right)^{-1.086} \tag{4}$$

$$c=\frac{\overline{v}}{\Gamma\left(1+\frac{1}{k}\right)} \tag{5}$$

3.4. Vertical Extrapolation of Wind Speed and Weibull Parameters at Different Heights

In this study, the wind shear model considered to extrapolate the wind profiles is the empirical power law. Equation (6) is therefore used to adjust the wind speeds measured at 10 m above the ground at hub heights of WT towers, as well as at some hilltops or exposed ridges [27] [28]:

$$V_{z}=V_{10}\left(\frac{z}{10}\right)^{\alpha} \tag{6}$$

With V_{10} the wind speed at the height of 10 m and V_z the speed at the height of z; z being the altitude.

α is the roughness coefficient defined by:

$$\alpha=0.37-0.088\ln\left(V_{10}\right) \tag{7}$$

On the other hand, k and c, respectively the Weibull scale factor and the shape parameters determined at 10 m height, are adjusted to any desired height as shown [29]:

$$C_{z}=C_{10}\left(\frac{z}{10}\right)^{n} \tag{8}$$

$$k_{z}=\frac{k_{10}}{1-0.00881\ln\left(z/10\right)} \tag{9}$$

k_z is the form factor at height z and C_z is the scale factor at height z.

The power law exponent n is given by:

$$n = \left[0.37 - 0.0088\ln(10)\right] \tag{10}$$

3.4.1. Wind Turbine Power Output and Capacity Factor

Each wind energy conversion system is designed to operate at its maximum efficiency within the rated wind speed and power. Therefore, once the Weibull scale and shape parameters are estimated, the performance of a wind turbine at a given location can be easily calculated using the average power and capacity factor. In this work, the electrical power of a wind turbine model is simulated using [30]-[32]:

$$P_e = \begin{cases} 0 & (v < v_d) \\ P_{en}\dfrac{v^k - v_d^k}{v_n^k - v_d^k} & (v_d \le v \le v_n) \\ P_{eR} & (v_n \le v \le v_c) \\ 0 & (v_c < v) \end{cases} \tag{11}$$

where:

P_{en} : rated electrical power;

v_d : wind turbine starting speed;

v_n : rated speed;

v_c : cut-off speed.

The output power of a wind turbine is given by the following relationship [23] [33]:

$$P_s = P_{en}\left\{\frac{e^{-\left(\frac{v_d}{C}\right)^k} - e^{-\left(\frac{v_n}{C}\right)^k}}{\left(\frac{v_n}{C}\right)^k - \left(\frac{v_d}{C}\right)^k} - e^{-\left(\frac{v_c}{C}\right)^k}\right\} \tag{12}$$

The capacity factor, which is described as the ratio between the average output power and the rated output power, is given by the following formula [34]:

$$C_f = \frac{P_S}{P_e} \tag{13}$$

3.4.2. Usable Wind Energy

The average usable (produced) wind energy is [35] [36]:

$$P_P = \eta P_u \tag{14}$$

With η the efficiency of the machine given by:

$$\eta = 2\frac{P_n}{\rho A v_n^3} \tag{15}$$

3.4.3. Daily Flow of Wind Pumping

The modeling of the wind pump is given by the equation below, highlighting, in

particular, the relationship between the flow, the head and the density of the fluid [34] [37]-[39].

$$Q = 3600 * 24 * \left(\frac{(\eta * P_u)}{(\rho_e * g * H)} \right) \tag{16}$$

with:

ρ_e: density of water (ρ_e = 1000 kg/m^3); g: the acceleration due to gravity (g = 9.81 m/s^2); H is the total head in m, and Q is the daily flow in m^3/day.

4. Results and Discussion

4.1. Average and Maximum Site Speed Curves

Figures 2-4 show the minimum and maximum speed curves for three study areas. We notice in Figure 2 that the maximum speed oscillates between 3 m/s and 5.8 m/s, and the maximum speed varies between 6.8 m/s and 12 m/s. Figure 3 shows the monthly evolution of the average and maximum speed of the city of Faya Largeau; the average speed varies between 4 m/s and 7 m/s, and the maximum speed oscillates between 10 m/s and 14 m/s. Figure 4 shows the average speed of Ounianga Kebir, which oscillates between 4 m/s and 7 m/s, and the maximum speed varies between 9 m/s and 12 m/s. All these figures show that the area of the Bodélé triangle benefits from a good wind speed.

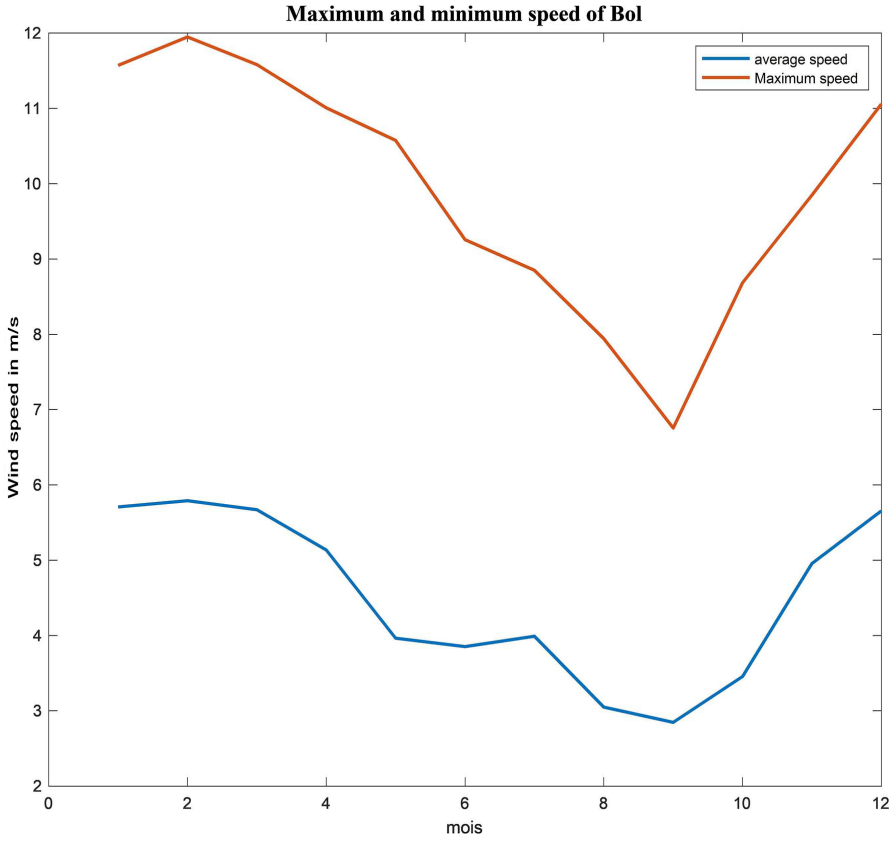

Figure 2. Average and maximum speed curve of Bol.

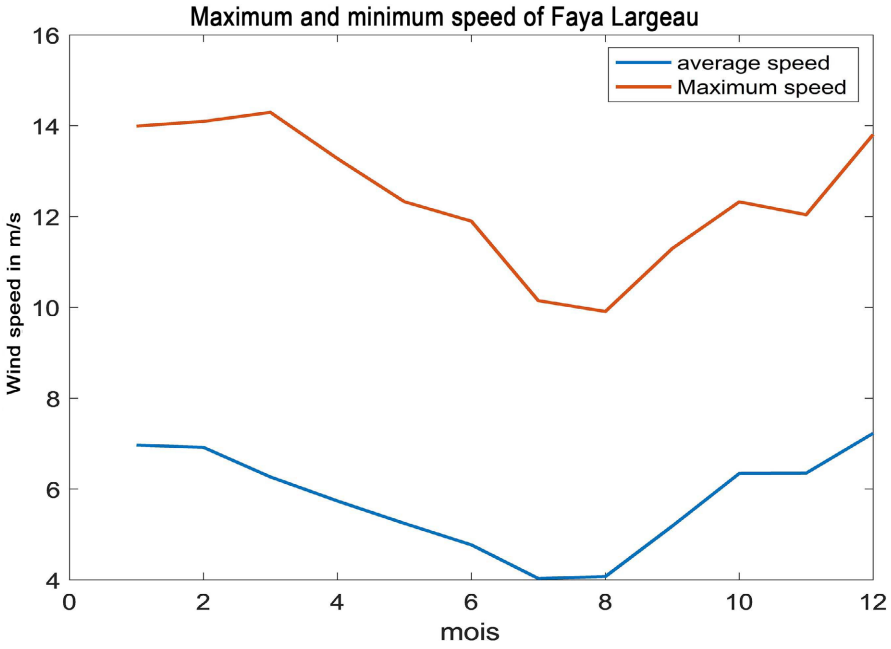

Figure 3. Average and maximum speed curve of Faya.

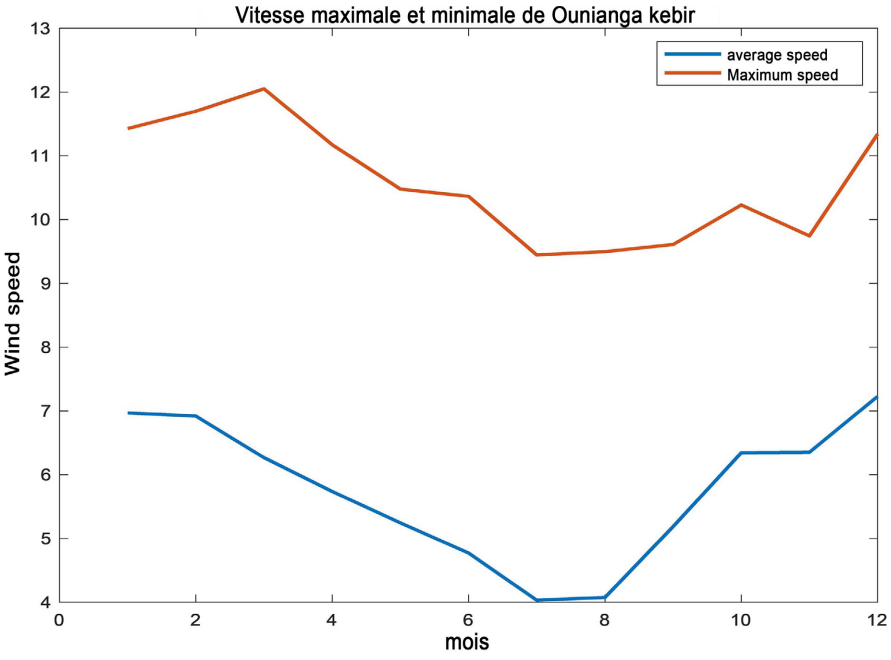

Figure 4. Average and maximum speed curve of Ounianga Kebir.

4.2. Hourly Variation in Wind Speed across the Different Zones and Monthly Values of the Weibull Parameters of the Different Cities

Figure 5 shows the different graphs of monthly wind speed changes for the study area for the month of January. We notice that for the city of Bol, the average speed varies between 4 m/s and 8 m/s. The windiest hours are from 8 a.m. to 2 p.m., where the average speed is greater than 6 m/s, and the minimum speed is observed

at 5 p.m. at 4.5 m/s.

For the city of Faya Largeau, we notice that the best windy hours are in the interval from 01:00 to 15:00, with an average above 10 m/s, with a peak of 14 m/s. The minimum speed is observed at 5 p.m. with a value of 9 m/s. We also notice that the hourly average wind speed is greater than 11 m/s.

The wind speed graph of the city of Ounianga Kebir shows an average that the speed of 9 m/s. We notice in the figure that the windiest hours are in the interval from 2 a.m. to 4 a.m. and from 7 a.m. to 2 p.m., with an average greater than 10 m/s. We also notice a drop in the wind speed at 5 p.m., the value of which is 6 m/s. Table 2 presents the monthly Weibull shape (k) and scale (c) parameters for Bol, Faya Largeau, and Ounianga Kebir. All three sites exhibit seasonal variations, with generally higher wind speeds from December to February and lower speeds during summer. Faya Largeau has the highest scale parameter, reaching 8.14 m/s in December, whereas Bol records the lowest value (3.20 m/s) in September. The shape parameter also varies seasonally, indicating changes in wind speed variability. Bol shows its lowest k value in September (1.64), suggesting greater variability than at the other sites during that month. These results highlight spatial and seasonal differences.

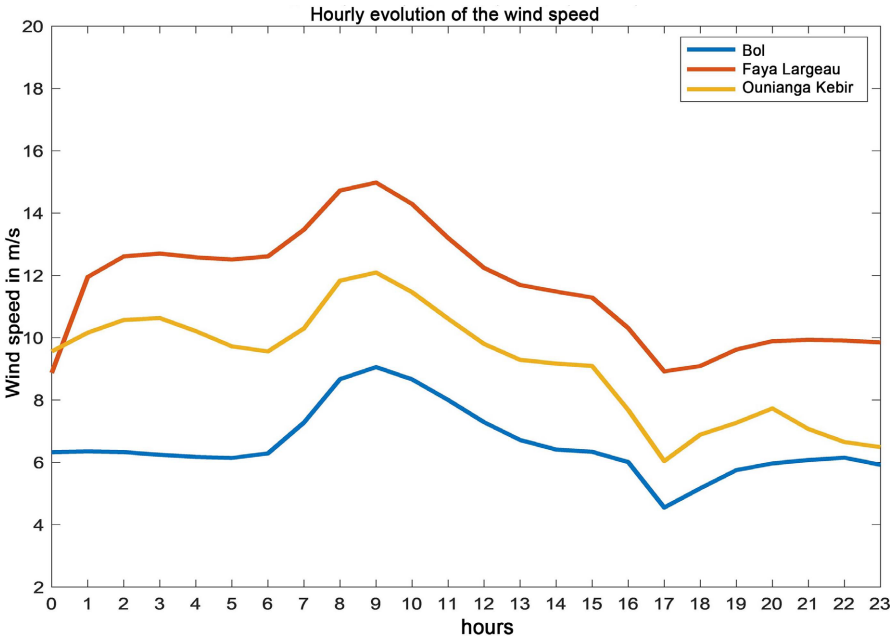

Figure 5. Hourly variations in average wind speeds in the study area.

Table 2. Monthly values of the Weibull parameters of the different cities.

		Bol	Faya Largeau	Ounianga Kebir
January	k	2.34	2.56	2.33
	c	6.44	7.85	6.32

Continued

February	k	2.36	2.55	2.34
	c	6.53	7.79	6.39
March	k	2.34	2.45	2.28
	c	6.40	7.07	6.04
April	k	2.23	2.35	2.20
	c	5.79	6.48	5.61
May	k	1.97	2.26	2.15
	c	4.47	5.91	5.33
June	k	1.94	2.16	2.15
	c	4.34	5.39	5.35
July	k	1.98	2.00	2.04
	c	4.51	4.55	4.76
August	k	1.71	2.00	2.03
	c	3.42	4.59	4.73
September	k	1.64	2.24	2.25
	c	3.20	5.82	5.89
October	k	1.83	2.46	2.31
	c	3.88	7.15	6.25
November	k	2.20	2.46	2.22
	c	5.60	7.16	5.71
December	k	2.33	2.60	2.35
	c	6.38	8.14	6.47

4.3. Curves of the Weibull and Rayleigh Statistical Distributions of the Study Area

Figures 6-8 represent the probability densities of the study area. The Weibull parameter values give us for the city of Bol, with the annual average speed of 4.51 m/s, $k = 2.10$ and $c = 5.09$ m/s. For the city of Faya Largeau, the average speed is 5.75 m/s, the shape parameter $k = 2.38$ and the scale factor $c = 6.49$ m/s. Finally, for the city of Ounianga Kebir, the average speed $v = 5.08$ m/s, $k = 2.22$ and $c = 5.73$ m/s. We notice that the different values of the shape parameters oscillate around 2, which shows that the Rayleigh distribution is well suited for this area. Figure 6 shows the Weibull distribution of the three cities in the Bodélé triangle area. It shows that for the three cities, the speed distributions are spread out with good speed bandwidths. There is also a low speed dispersion in the three with a standard deviation value oscillating between 0.51 and 1.1. The maximum proba-

bility densities oscillate between 0.14 and 0.17. The values of the shape parameters oscillate around 2. Figure 7 presents the Rayleigh velocity distributions of the three sites. Given the importance of the speed in the area, this distribution is well suited for the characterization of the wind on the site. Figure 8 presents the Weibull cumulative distribution.

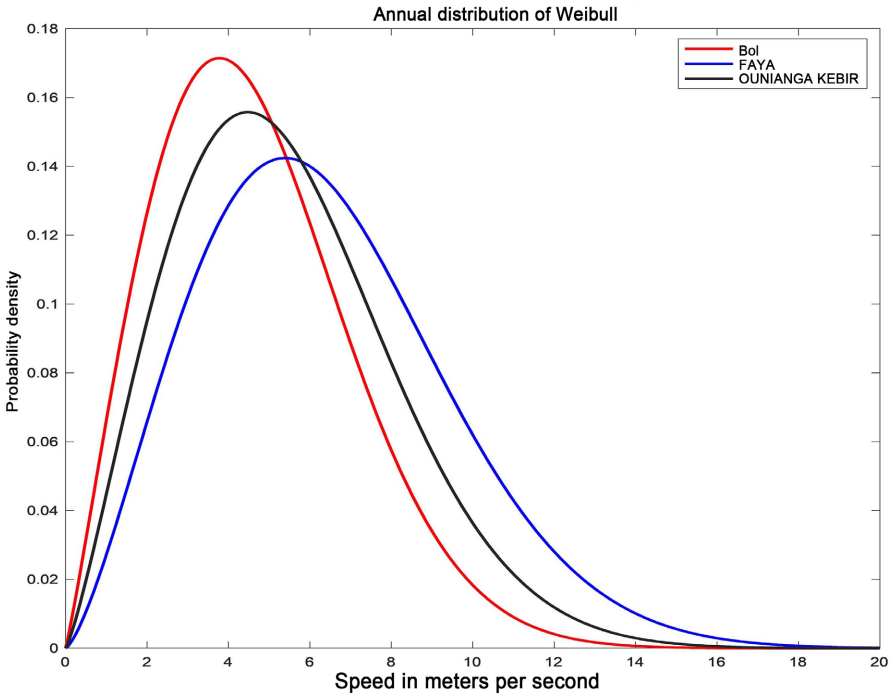

Figure 6. Distribution de Weibull.

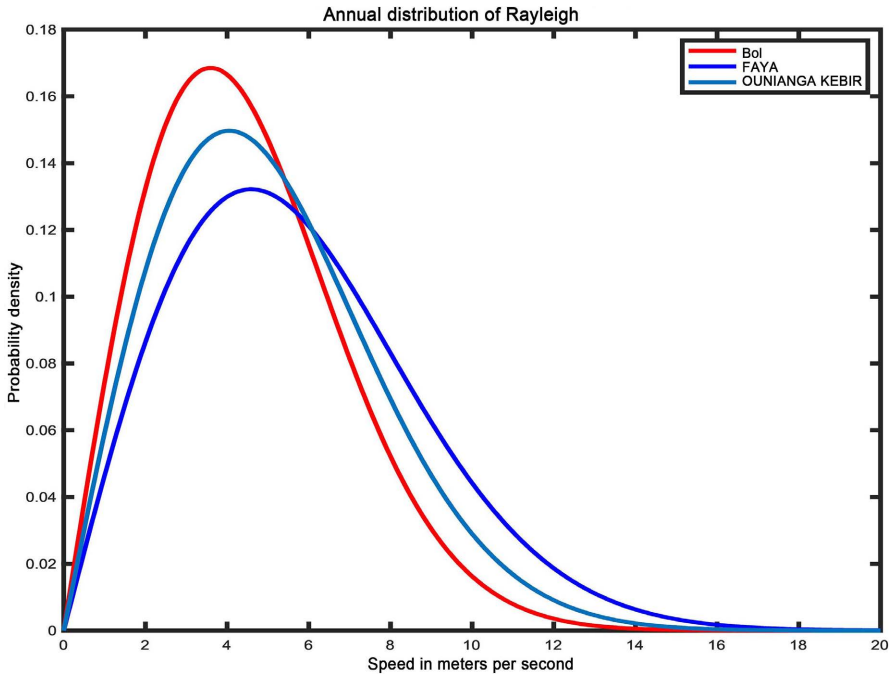

Figure 7. Annual distribution of Rayleigh.

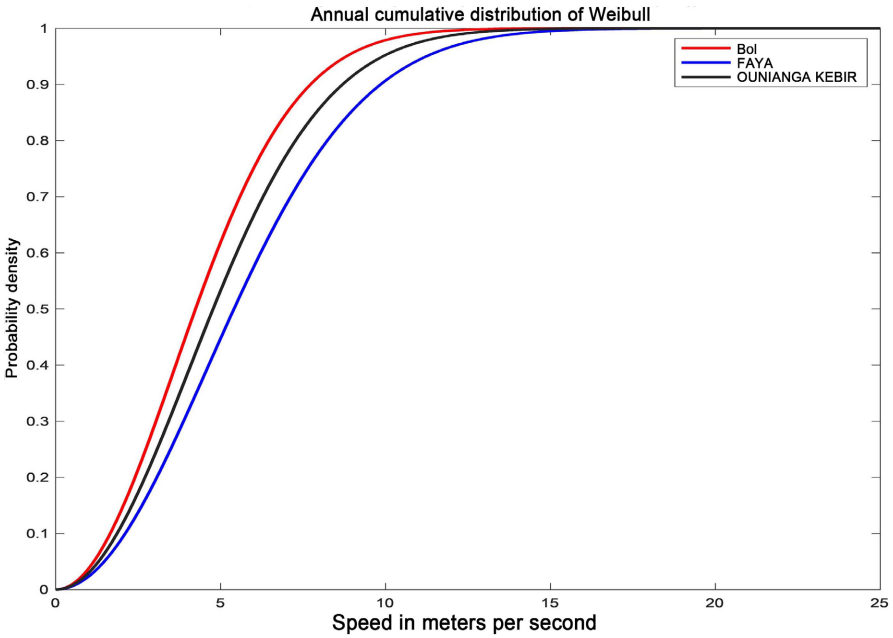

Figure 8. cumulative distribution of Weibull.

5. Application to the Pumping from Different Wind Turbines

Table 3 presents the technical characteristics of the three wind turbines considered for the Bodélé Triangle in Chad. The AN Bonus 1 MW and HSW 1000/57 turbines have the same rated power and hub height, but the latter has a larger rotor and a lower rated wind speed, which may improve energy capture at moderate wind speeds. The Vestas 2 MW/80 has the largest rotor and rated power, offering greater potential energy production, although it reaches rated power at a higher wind speed. All three turbines have a cut-in speed of 4 m/s and a cut-out speed of 25 m/s. Their selection enables a comparison of turbine sizes and performance under the wind conditions observed in the study area. The final choice should be based on turbine power curves, wind speeds at hub height, and suitability for the region's dusty and hot conditions.

Table 3. Characteristics of wind turbines.

Wind turbine	Starting speed	Rated speed	Stop speed	Rated power	Rotor diameter	mast height
AN Bonus 1 MW	4 m/s	15 m/s	25 m/s	1000 KW	46 m	70 m
HSW 1000/57	4 m/s	13 m/s	25 m/s	1000 KW	57 m	70 m
Vestas 2 MW/80	4 m/s	16 m/s	25 m/s	2 MW	80 m	67 m

5.1. Vertical Extrapolation of Velocities and Weibull Parameters at the Height of Wind Turbines

As the speed varies with altitude and the height of the mast of a wind turbine being one of its characteristics, we evaluated the speed at the height of each wind turbine

by the relationship (9), the roughness coefficient by the relationship (10), the shape parameters and the scale factor by the relations (11) and (12). The results are presented in Table 4.

Table 4. Extrapolation of Weibull parameters to the height of wind turbines.

	Bol	Faya Largeau	Ounianga Kebir
V at 10 m in (m/s)	4.51	5.75	5.08
K at 10 m	2.10	2.38	2.22
C at 10 m in (m/s)	5.09	6.49	5.73
V at 67 m in (m/s)	9.03	11.29	10.00
K at 67 m	2.14	2.42	2.26
C at 67 m in (m/s)	10.19	12.74	11.27
V at 70 m in (m/s)	9.17	11.46	10.15
K at 70 m	2.14	2.42	2.26
C at 70 m in (m/s)	10.35	12.93	11.44

5.2. Flow and Daily Power of Annual Average Wind Speeds

Tables 5-7 give the values of the electrical powers, the useful powers and the daily water flows according to the nominal power of each wind turbine. We notice that the electric power varies between 357.90 KW/m^2 to 901.24 KW/m^2 for the three cities. The maximum power is observed at the Faya Largeau site and the minimum at Bol. The useful power values for the three sites vary between 876.16 KW/m^2 to 3586.5 KW/m^2. The daily water flows of each wind turbine, in turn, vary from 48,916 m^3/day and 109,100 m^3/day.

Table 5. Power and daily flow for the city of Bol.

Wind turbine	Electrical power	Useful power	Daily flow
AN Bonus 1 MW	357.90 KW/m^2	876.16 KW/m^2	48,916 m^3/day
HSW 1000/57	357.90 KW/m^2	1345.3 KW/m^2	48,916 m^3/day
Vestas 2 MW/80	622.90 KW/m^2	2528.6 KW/m^2	76,920 m^3/day

Table 6. Power and daily flow for the city of Faya Largeau.

Wind turbine	Electrical power	Useful power	Daily flow
AN Bonus 1 MW	600.97 KW/m^2	2757.2 KW/m^2	154,010 m^3/day
HSW 1000/57	600.97 KW/m^2	1795.7 KW/m^2	154,010 m^3/day
Vestas 2 MW/80	901.24 KW/m^2	5184 KW/m^2	157,690 m^3/day

Table 7. Power and daily flow for the city of Ounianga Kebir.

Wind turbine	Electrical power	Useful power	Daily flow
AN Bonus 1 MW	519.38 KW/m^2	1242.5 KW/m^2	106,570 m^3/day
HSW 1000/57	519.38 KW/m^2	1907.8 KW/m^2	106,570 m^3/day
Vestas 2 MW/80	751.89 KW/m^2	3586.5 KW/m^2	109,100 m^3/day

5.3. Wind Turbine Capacity Factor for the Study Area

Figure 9 presents the monthly evolutions of the different curves of the capacity factor of three wind turbines in each of the towns in the study area. We find that for the city of Bol, the capacity factor oscillates between 0.18 and 0.60 for all wind turbines. We also observe manual oscillations of the capacity factors with minimum values between May and October. The maximum capacity values are observed from November to April. The wind turbine that presents the best values of the capacity factor is HSW 1000/57 with values that vary from 0.22 to 0.60.

For the Faya Largeau site, the values of the capacity factors oscillate around 0.26 to 0.71, for three aerogenerators. We note on the curves that the values of the capacity factors are greater than 0.50 from October to June, *i.e.*, 9 months in the year. This demonstrates that the Faya Largeau site is very suitable for wind power installations. The most productive wind turbine in terms of capacity factor is HSW 1000/57 with values ranging from 0.37 to 0.71, followed by the AN Bonus 1 MW wind turbine with values ranging from 0.30 to 0.62. The least productive wind turbine in terms of capacity factor is VestasMW/80 with values ranging from 0.26 to 0.46.

Finally, for the Ounianga Kebir site, the capacity factors for the three wind turbines vary between 0.28 and 0.60. We note an annual variation as for the other sites of the capacity factor. We also note that all values are greater than 0.26, which corresponds to the capacity factor standard for the operation of a wind turbine on a site.

Figure 10 shows us the electrical power produced by the wind turbine for the different towns in the study area. Graph 1 shows us the monthly evolution of the electrical power produced by the various wind turbines on the Bol site. We notice on these curves that the Vesta S2 MW/80 aerogenerator presents low power values, with values lower than 100 MW/m^2. The HSW 1000/57 and AN Bonus 1 MW wind turbines are the best on the site with electrical powers that vary from 180 MW/m^2 to 600 MW/m^2. Graph 2 shows the monthly curves of the electric power curves of the three wind turbines for the Faya Largeau site. A reading of the curve shows that the Vestas 2 MW/80 aerogenerator beats the power record, followed by HSW 1000/57, whose values vary from 400 MW/m^2 to 1200 MW/m^2. The curves in Graph 3 show the electrical power of the city of Ounianga Kebir. The power values oscillate between 400 MW/m^2 and 900 MW/m^2 for the Vestas 2 MW/80 and HSW 1000/57 aerogenerator. We notice that Vestas 2 MW/80 breaks the record in power.

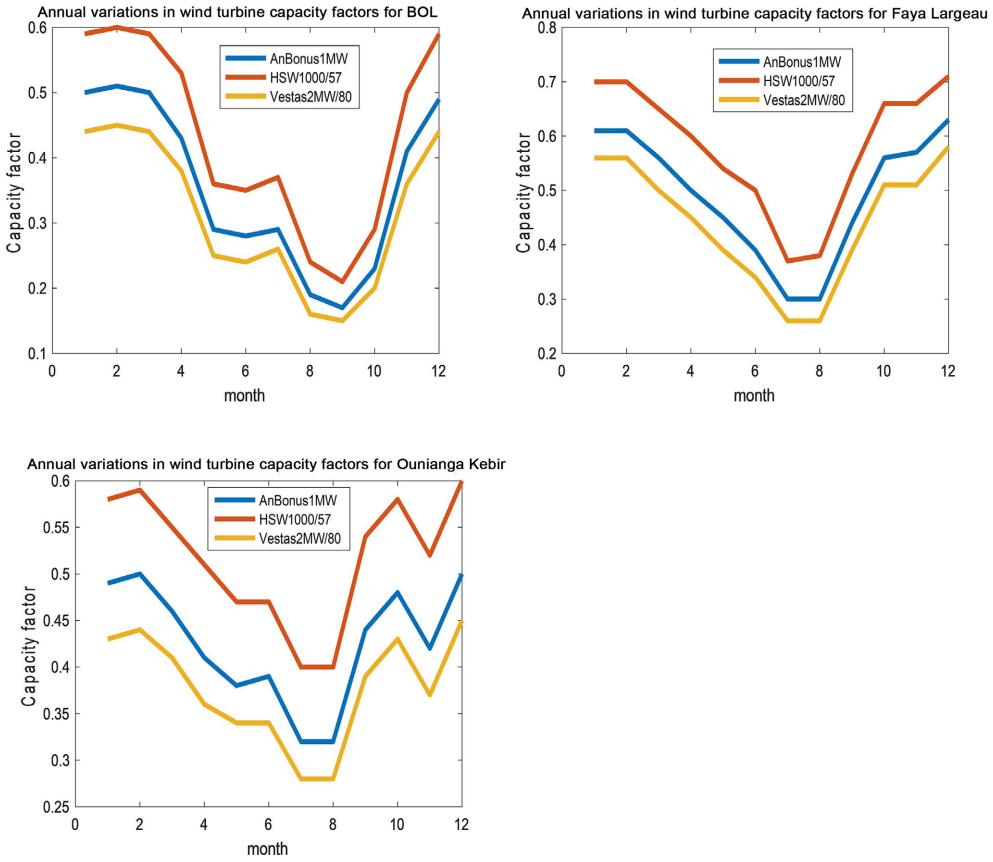

Figure 9. Monthly curves of wind turbine capacity factors.

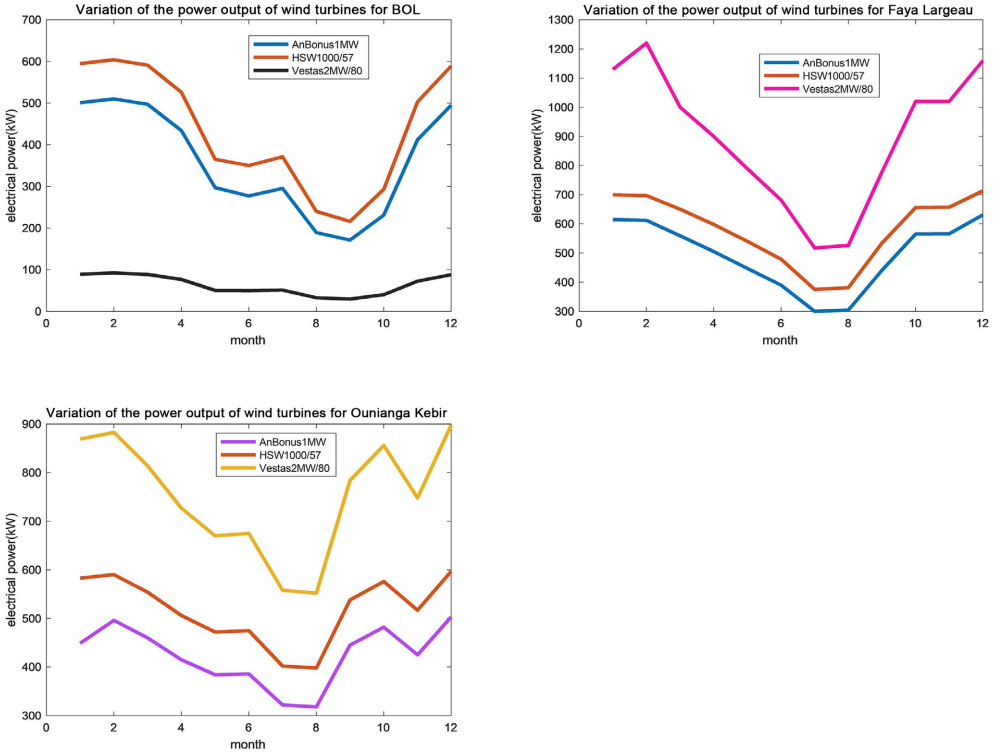

Figure 10. Electrical power curves of the various wind turbines.

5.4. Water Flows Produced by Aerogenerator

Figure 11 shows the daily water flows produced by aerogenerator. The daily flow strongly depends on the months. Flows are highest from November to April. We notice a drop in flows from May to October.

Graph 1 presents the curves of the monthly flows of the various wind turbines for the city of Bol. We read on this curve flows varying from 1970 m^3/day to 157,000 m^3/day. However, there is a monthly variation in flows. The wind turbine that breaks the record in daily throughput is HSW 1000/57 with a maximum throughput of 157,000 m^3/day in February and a minimum throughput of 1920 m^3/day in September, followed by the AN Bonus 1 MW wind turbine with a peak of 102,000 m^3/day in February and the minimum of 12,500 m^3/day in September.

Graph 2 presents the water flows for the city of Faya Largeau, we note a variation in water flows which oscillates between a maximum of 308,000 m^3/day to a minimum of 35,100 m^3/day. The most productive wind turbine is Vestas 2 MW/80 with a maximum flow of 308,000 m^3/day and a minimum of 55,100 m^3/day followed by the HSW 1000/57 wind turbine with a maximum flow of 196,000 m^3/day and a minimum of 35,100 m^3/day.

Graph 3 represents the daily water flows of the city of Ounianga Kebir. We find that the maximum flow is 156,000 m^3/day and the minimum flow is 39,400 m^3/day. The most productive aerogenerator is Vestas 2 MW/80 with a maximum flow of 156,000 m^3/day and a minimum of 61,900 m^3/day.

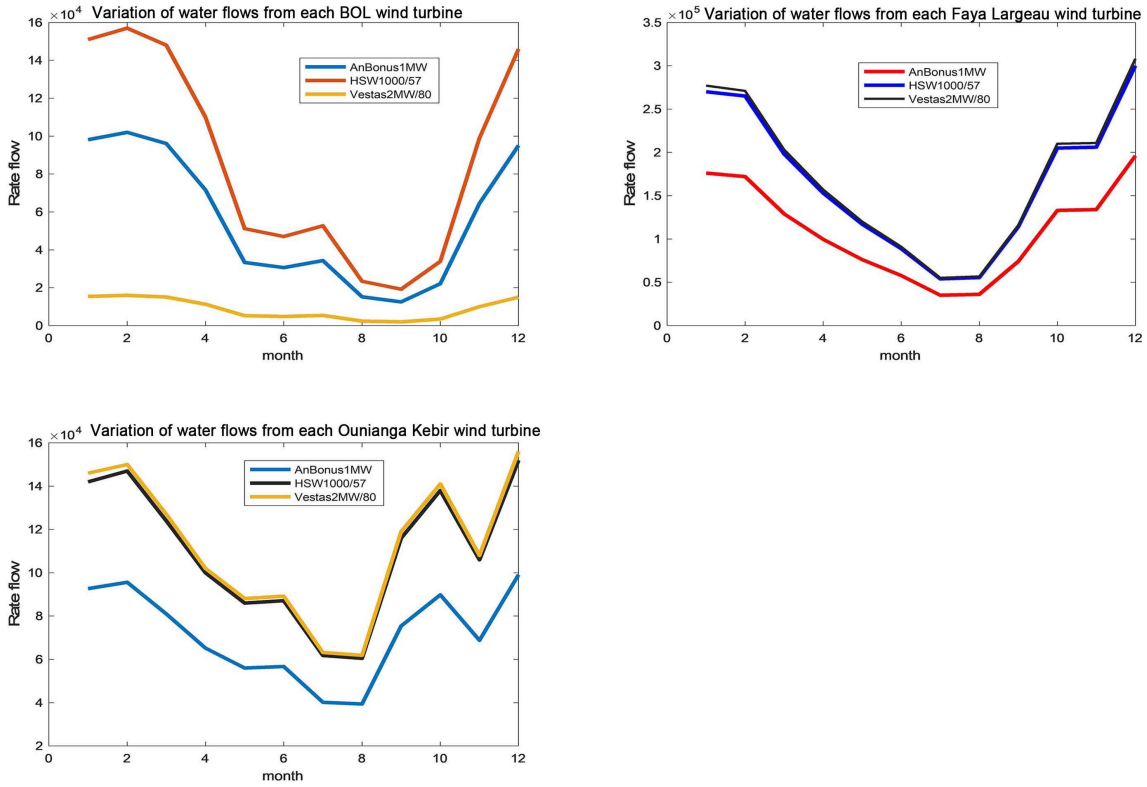

Figure 11. Curves of monthly daily flows of wind turbines for each city.

6. Application of the Rayleigh Distribution to Wind Pumping: Validation of Results

This section follows the same methodological approach as Section 4, using the Rayleigh distribution ($k = 2$) instead of the full Weibull distribution, in order to validate and compare the previously obtained results.

6.1. Vertical Extrapolation of Rayleigh Parameters

The vertical extrapolation of the annual mean wind speeds shows a significant increase in wind resource availability with altitude for the three sites under study, presented in Table 8. It can be observed that at a height of 70 m, the mean wind speed nearly doubles compared to that measured at 10 m, increasing from 4.51 to 9.17 m/s for Bol, from 5.75 to 11.46 m/s for Faya Largeau, and from 5.08 to 10.15 m/s for Ounianga Kebir. This evolution confirms the critical importance of the mast height selection in the design of wind energy installations in Sahelian regions.

Table 8. Extrapolation of Rayleigh distribution parameters at wind turbine hub heights.

	Bol	Faya Largeau	Ounianga Kebir
V at 10 m	4.51	5.75	5.08
k at 10 m	2	2	2
C at 10 m	5.09	6.49	5.73
V at 67 m	9.03	11.29	10.00
k at 67 m	2	2	2
C at 67 m	**10.19**	**12.74**	**11.28**
V at 70 m	9.17	11.46	10.15
k at 70 m	2	2	2
C at 70 m	**10.35**	**12.93**	**11.45**

It should be noted that the shape parameter k remains fixed at 2 at all heights, consistent with the Rayleigh distribution assumption, while the scale factor C follows the same evolution law as the mean wind speed. The ranking of the sites is preserved regardless of the altitude considered: Faya Largeau > Ounianga Kebir > Bol, which reflects a consistency in the relative wind potential of the three cities independent of the chosen mast height. These results are in close agreement with those previously obtained using the full Weibull distribution, confirming the suitability of the Rayleigh model for this study area.

6.2. Capacity Factor and Output Power

The results obtained using the Rayleigh distribution confirm the trends already observed with the full Weibull distribution, presented in Table 9. For all three

sites, the HSW 1000/57 wind turbine consistently exhibits the highest capacity factor (0.456 at Bol, 0.572 at Faya Largeau, and 0.514 at Ounianga Kebir), followed by the AN Bonus 1 MW, while the Vestas 2 MW/80 shows the lowest capacity factors despite its higher rated power (2 MW). This apparent contradiction is explained by the higher cut-in and rated speeds of the Vestas 2 MW/80 (16 m/s versus 13 m/s for the HSW 1000/57), which restrict its optimal operation to the strongest wind regimes, statistically less frequent even on well-exposed sites such as Faya Largeau.

Table 9. Capacity factor and output power of wind turbines according to the Rayleigh distribution.

Ville	Éolienne	Chub (m/s)	C_f	P_s (kW)
Bol	AN Bonus 1 MW	10.35	0.376	375.8
	HSW 1000/57	10.35	0.456	455.5
	Vestas 2 MW/80	10.19	0.332	663.5
Faya Largeau	AN Bonus 1 MW	12.93	0.495	494.8
	HSW 1000/57	12.93	0.572	571.5
	Vestas 2 MW/80	12.74	0.452	903.4
Ounianga Kebir	AN Bonus 1 MW	11.45	0.434	434.1
	HSW 1000/57	11.45	0.514	513.9
	Vestas 2 MW/80	11.28	0.389	778.6

In terms of absolute power output (Ps), however, the Vestas 2 MW/80 remains the most productive turbine at all three sites (663.5 kW at Bol, 903.4 kW at Faya Largeau, and 778.6 kW at Ounianga Kebir), owing to its considerably larger swept area, which compensates for a lower capacity factor. This result highlights the importance of jointly considering both the capacity factor and the absolute power output when selecting a wind turbine suited to a given site.

Faya Largeau again confirms its position as the most favorable site for wind energy development, with capacity factors exceeding 0.45 for all three turbine models tested, well above the commonly accepted profitability threshold of 0.25 - 0.30.

6.3. Available Power Density and Usable Power

The available wind power density (P_u) varies significantly across sites, ranging from 0.862 to 0.903 kW/m^2 at Bol, 1.683 to 1.761 kW/m^2 at Faya Largeau, and 1.169 to 1.222 kW/m^2 at Ounianga Kebir, in Table 10. These values, calculated at the respective hub heights of each turbine (67 m for the Vestas 2 MW/80 and 70 m for the other two models), illustrate that Faya Largeau possesses an energy potential nearly twice that of Bol, consistent with the higher mean wind speeds recorded at that site.

Table 10. Available power density and usable power at hub heights (Rayleigh distribution).

Ville	Hauteur moyeu	P_u (kW/m²)	P_p An Bonus	P_p HSW	P_p Vestas
Bol	70/67 m	0.903/0.862	0.263	0.263	0.137
Faya Largeau	70/67 m	1.761/1.683	0.512	0.513	0.267
Ounianga Kebir	70/67 m	1.222/1.169	0.356	0.356	0.185

The usable power (P_p), which incorporates the conversion efficiency specific to each turbine type (η), confirms the hierarchy observed above. Since the AN Bonus 1 MW and HSW 1000/57 share identical efficiencies ($\eta = 0.291$), which are higher than that of the Vestas 2 MW/80 ($\eta = 0.159$), these two turbines display nearly identical usable power densities at each site, whereas the Vestas 2 MW/80 shows markedly lower values (0.137 to 0.267 kW/m²), despite its higher rated capacity.

This result demonstrates that the conversion efficiency (η), directly linked to the ratio of rated power to the cube of rated wind speed, constitutes a decisive parameter in evaluating the exploitable energy potential, independent of turbine size.

6.4. Daily Pumping Flow Rates

The daily flow rates calculated for a total pumping head of H = 50 m reveal considerable wind pumping potential at all three sites, ranging from 76,990 m³/day (Bol, AN Bonus 1 MW) to 236,460 m³/day (Faya Largeau, Vestas 2 MW/80), presented in Table 11.

Table 11. Total usable power and daily flow rates of wind pumping for a total head H = 50 m.

Villes	Wind Turbine	P_p (kW/m²)	$P_p \cdot A$ (kW)	Q (m³/day)
Bol	AN Bonus 1 MW	0.263	437.1	76,990
	HSW 1000/57	0.263	671.1	118,220
	Vestas 2 MW/80	0.137	688.6	121,300
Faya Largeau	AN Bonus 1 MW	0.512	850.9	149,900
	HSW 1000/57	0.513	1309.1	230,640
	Vestas 2 MW/80	0.267	1342.1	236,460
Ounianga Kebir	AN Bonus 1 MW	0.356	591.6	104,240
	HSW 1000/57	0.356	908.4	160,020
	Vestas 2 MW/80	0.185	929.9	163,810

The ranking of sites in terms of flow rate faithfully reproduces that obtained for total usable power, with Faya Largeau ranking first, followed by Ounianga Kebir and then Bol. This hierarchy confirms the wind resource gradient identified across the entire study area, with Faya Largeau benefiting from the highest wind speeds throughout the year.

Regarding turbine selection, it is observed that despite its lower capacity factor, the Vestas 2 MW/80 systematically generates the highest flow rates at all three

sites (121,300 m^3/day at Bol, 236,460 m^3/day at Faya Largeau, and 163,810 m^3/day at Ounianga Kebir), owing to its considerably larger swept area (5026.6 m^2 compared to 2551.8 m^2 for the HSW 1000/57 and 1661.9 m^2 for the AN Bonus 1 MW).

It is also worth noting that the HSW 1000/57 and Vestas 2 MW/80 exhibit relatively close flow rates at all three sites (differences of 3% - 12%), suggesting that for pumping applications where investment cost is a determining factor, the HSW 1000/57 could represent a more economically advantageous alternative, with a potentially more favorable performance-to-cost ratio.

These results demonstrate the strong potential of wind pumping for agricultural and domestic water supply in the Bodélé triangle region, particularly at the Faya Largeau site, which could provide, with a single Vestas 2 MW/80 turbine, a daily water volume sufficient to irrigate several hundred hectares or supply a substantial population with drinking water.

7. The Wind Roses of the Study Area

Figures 12-14 respectively present the wind rose diagrams of the triangle area. At first glance, we notice that the prevailing wind on the three sites is from the East-North-East sector. The maximum frequencies are as follows: 55% for the town of Bol, 85% for the town of Faya Largeau and 70% for the town of Ounianga Kebir. We also notice that the frequency of calm winds is zero on the set of three. This justifies the violent nature of the wind in the area. Given the zero frequency of the calm wind, we conclude that the hybrid Weibull distribution is not suitable for characterizing the wind in this area.

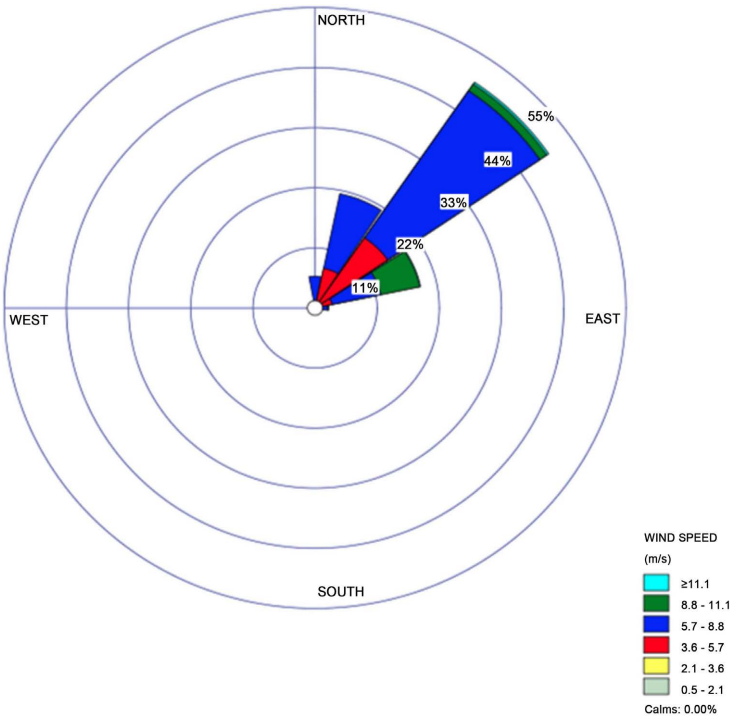

Figure 12. Wind rose diagram of Bol.

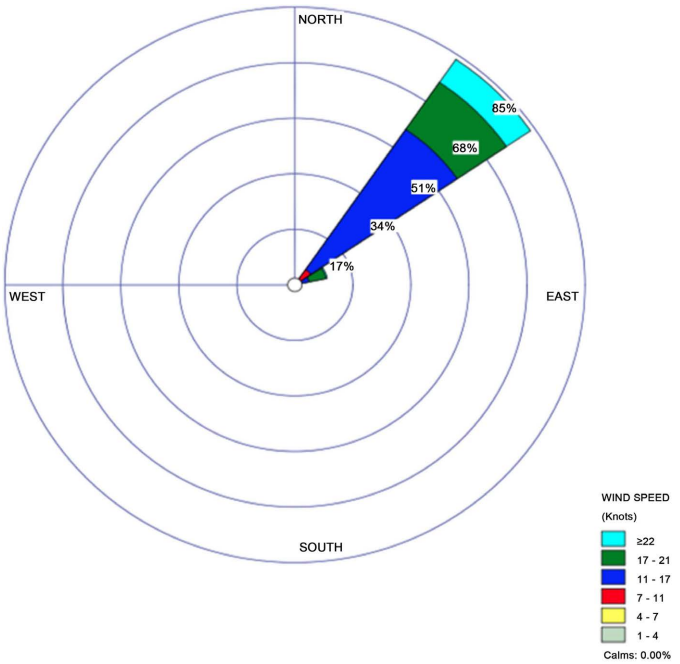

Figure 13. Wind rose diagram of Faya Largeau.

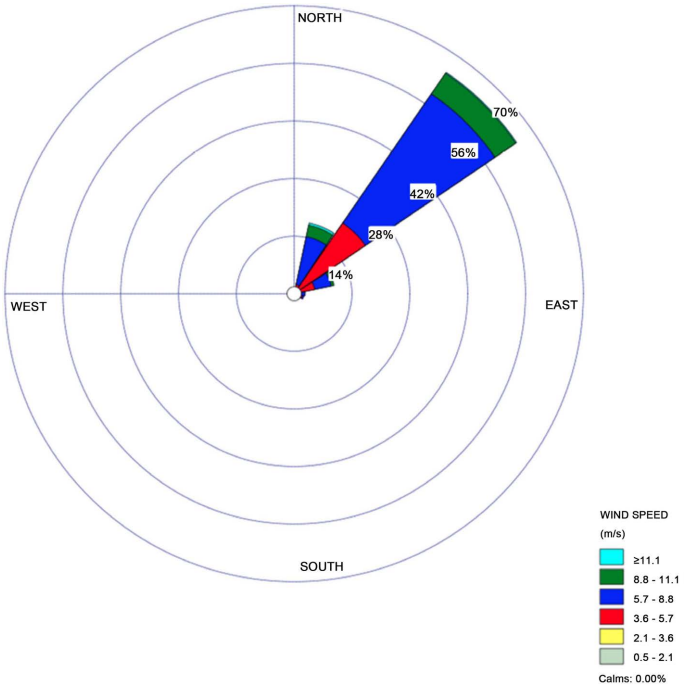

Figure 14. Wind rose diagram of Ounianga Kebir.

8. Conclusions

Water being an essential element for life, its exploitation generally requires energy. Chad, a country strongly exposed to the effects of climate change, faces a population increasingly confronted with drought and declining agropastoral yields. The Bodélé triangle stands out for the violence of its wind regime, a resource that

offers interesting prospects for groundwater exploitation in this predominantly arid area. The results show considerable wind potential across the three sites studied: the annual wind speed at 10 m exceeds 4.5 m/s everywhere, and reaches more than 9 m/s at the height of the various wind turbines. The application to pumping reveals daily flow rates ranging from 48,916 to 157,690 m^3/day depending on the site and turbine type, with a marked seasonal variation (maximum flows from November to April). The HSW 1000/57 and Vestas 2 MW/80 turbines stand out as the most efficient, respectively in terms of capacity factor and absolute flow rate. The use of the Rayleigh distribution, alongside the Weibull distribution, confirmed these results with deviations below 5%, statistically validating its suitability for characterizing wind behavior in this area. Furthermore, the wind roses revealed a dominant East-North-East direction as well as a zero frequency of calm winds at all three sites, confirming the violent and persistent nature of the wind and ruling out the use of the hybrid Weibull distribution.

In light of these results, the Bodélé triangle area presents a satisfactory wind potential that can serve as a concrete response to the many challenges posed by climate change, particularly regarding access to water for agriculture and local populations.

Author Contributions

- **Fia Oung-Zetna:** Conceptualized the study, developed the methodology, analyzed the data, and wrote the main manuscript draft.
- **Zoutchibé Joseph:** Collected, curated, and pre-processed the wind speed datasets for the Bodélé Triangle region.
- **Gotoum Nadjinangar:** Contributed to the statistical calculation of Weibull parameters and the validation of the mathematical models.
- **Laleko Benjamin:** Performed the software simulations, generated the wind rose diagrams, and formatted the visual results.
- **Foulla Dieudonné Platou:** Assisted in the geographical contextualization, technical interpretation of results, and manuscript editing.
- **Noel Djongyang:** Supervised the research project, guided the methodology, and critically reviewed the final manuscript.

Conflicts of Interest

The authors declare no conflicts of interest regarding the publication of this paper.

References

[1] Keyhani, A., Ghasemi-Varnamkhasti, M., Khanali, M. and Abbaszadeh, R. (2010) An Assessment of Wind Energy Potential as a Power Generation Source in the Capital of Iran, Tehran. *Energy*, **35**, 188-201. https://doi.org/10.1016/j.energy.2009.09.009

[2] Soulouknga, M.H., Doka, S.Y., Revanna, N., Djongyang, N. and Kofane, T.C. (2018) Analysis of Wind Speed Data and Wind Energy Potential in Faya-Largeau, Chad, Using Weibull Distribution. *Renewable Energy*, **121**, 1-8. https://doi.org/10.1016/j.renene.2018.01.002

[3] Zghal, W., Kantchev, G. and Kchaou, H. (2009) Optimisation technico-économique d'un système énergétique éolien pour une maison familiale. https://www.academia.edu/download/7303162/cere_wc_4.pdf

[4] Soulouknga, M.H., Kidmo Kaoga, D., Djongyang, N. and Yamigno Doka, S. (2023) Comparaison du potentiel énergétique éolien des trois zones climatiques du Tchad. *Journal of Renewable Energies*, **19**, 49-58. https://doi.org/10.54966/jreen.v19i1.547

[5] Belaraissia, I. (2023) Conception et réalisation d'un système de transmission pour une éolienne de pompage d'eau. Ph.D. Thesis, Larbi Tebessi University. http://dspace.univ-tebessa.dz:8080/jspui/handle/123456789/10522

[6] Lievin, Y.M.N. (2022) Etude d'impact financier du pompage d'eau douce de la rivière Oubangi en RD Congo vers le lac Tchad dans le projet d'investissement de la ligne électrique 400 kV Inga-Moanda-Cabinda-Pointe-Noire. *International Journal of Innovation and Applied Studies*, **36**, 219-221. https://search.proquest.com/openview/8fc93946548521e16ea0ede06924ea31/1?pq-origsite=gscholar&cbl=2031961

[7] Bellarbi, S. (2015) Estimation technico-économique de la production d'électricité par voie éolienne, intégrée aux réseaux interconnectés de transport électrique. Ph.D. Thesis, Université de Tlemcen-Abou Bekr Belkaid. https://www.pnst.cerist.dz/detail.php?id=78636/

[8] Tardy, A. (2022) Conception d'un stockage d'énergie éolienne pour une entreprise minière isolée du réseau: Faisabilité du stockage par pompage hydraulique. Ph.D. Thesis, École de technologie supérieure. https://espace.etsmtl.ca/id/eprint/3112/

[9] Lienou, G. (2025) Vers une approche globale de la gestion de la ressource comme solution aux crises d'eau des dernières décennies au Cameroun. https://www.academia.edu/download/80362798/iahs_274_337.pdf

[10] Bétinbaye, Y. (2025) Pollution des eaux du fleuve Chari et incidences sociales dans la ville de Sarh au sud du Tchad. In: Bétinbaye, Y., Mbaye, N.G. and Michel, T., Eds., *Géopolitique Mondiale*, 67.

[11] Guebsi, R. and Chokmani, K. (2025) Effects of Large- and Meso-Scale Circulation on Uprising Dust over Bodélé in June 2006 and June 2011. *Remote Sensing*, **17**, 2674. https://doi.org/10.3390/rs17152674

[12] Ali, E., Xu, W., Xie, L. and Ding, X. (2022) Assessment of Aeolian Activity in the Bodélé Depression, Chad: A Dense Spatiotemporal Time Series from Landsat-8 and Sentinel-2 Data. *Frontiers in Environmental Science*, **9**, Article ID: 808802. https://doi.org/10.3389/fenvs.2021.808802

[13] Washington, R. and Todd, M.C. (2005) Atmospheric Controls on Mineral Dust Emission from the Bodélé Depression, Chad: The Role of the Low Level Jet. *Geophysical Research Letters*, **32**, 2005GL023597. https://doi.org/10.1029/2005gl023597

[14] Bristow, C.S., Drake, N. and Armitage, S. (2009) Deflation in the Dustiest Place on Earth: The Bodélé Depression, Chad. *Geomorphology*, **105**, 50-58. https://doi.org/10.1016/j.geomorph.2007.12.014

[15] Washington, R., Todd, M.C., Engelstaedter, S., Mbainayel, S. and Mitchell, F. (2006) Dust and the Low-Level Circulation over the Bodélé Depression, Chad: Observations from BoDEx 2005. *Journal of Geophysical Research*: *Atmospheres*, **111**, 2005JD006502. https://doi.org/10.1029/2005jd006502

[16] Abouchami, W., Näthe, K., Kumar, A., Galer, S.J.G., Jochum, K.P., Williams, E., *et al.* (2013) Geochemical and Isotopic Characterization of the Bodélé Depression Dust Source and Implications for Transatlantic Dust Transport to the Amazon Basin. *Earth and Planetary Science Letters*, **380**, 112-123.

https://doi.org/10.1016/j.epsl.2013.08.028

[17] Serban, A., Paraschiv, L.S. and Paraschiv, S. (2020) Assessment of Wind Energy Potential Based on Weibull and Rayleigh Distribution Models. *Energy Reports*, **6**, 250-267. https://doi.org/10.1016/j.egyr.2020.08.048

[18] Kwon, S. (2010) Uncertainty Analysis of Wind Energy Potential Assessment. *Applied Energy*, **87**, 856-865. https://doi.org/10.1016/j.apenergy.2009.08.038

[19] Chaurasiya, P.K., Kumar, V.K., Warudkar, V. and Ahmed, S. (2021) Evaluation of Wind Energy Potential and Estimation of Wind Turbine Characteristics for Two Different Sites. *International Journal of Ambient Energy*, **42**, 1409-1419. https://doi.org/10.1080/01430750.2019.1611634

[20] Düzcan, A. and Kara, Y.A. (2025) Assessment of Wind Energy Potential: A Case Study. *Energy Sources, Part A: Recovery, Utilization, and Environmental Effects*, **47**, 6045-6061. https://doi.org/10.1080/15567036.2021.1903119

[21] Fyrippis, I., Axaopoulos, P.J. and Panayiotou, G. (2010) Wind Energy Potential Assessment in Naxos Island, Greece. *Applied Energy*, **87**, 577-586. https://doi.org/10.1016/j.apenergy.2009.05.031

[22] Wang, Z. and Liu, W. (2021) Wind Energy Potential Assessment Based on Wind Speed, Its Direction and Power Data. *Scientific Reports*, **11**, Article No. 16879. https://doi.org/10.1038/s41598-021-96376-7

[23] Kidmo, D.K., Bogno, B., Deli, K., Aillerie, M. and Ngoussandou, B.P. (2021) Economic Assessment of WECS for Water Pumping Systems in the North Region of Cameroon. *Renewable Energy and Environmental Sustainability*, **6**, Article 6. https://doi.org/10.1051/rees/2021006

[24] Saeed, T.M. (2020) Sustainable Energy Potential in Sudan. *Journal of Engineering and Computer Science* (*JECS*), **20**, 1-10. https://www.researchgate.net/profile/Eisa-M-Tayeb/publication/362668611_Renewable_Energy_Sustainable_in_Sudan/links/62f7869379550d6d1c78fc8c/Renewable-Energy-Sustainable-in-Sudan.pdf

[25] Safari, B. and Gasore, J. (2010) A Statistical Investigation of Wind Characteristics and Wind Energy Potential Based on the Weibull and Rayleigh Models in Rwanda. *Renewable Energy*, **35**, 2874-2880. https://doi.org/10.1016/j.renene.2010.04.032

[26] Celik, A.N. (2004) A Statistical Analysis of Wind Power Density Based on the Weibull and Rayleigh Models at the Southern Region of Turkey. *Renewable Energy*, **29**, 593-604. https://doi.org/10.1016/j.renene.2003.07.002

[27] Rostami, S., Rostamzadeh, H. and Fatehi, R. (2021) A New Wind Turbine Driven Trigeneration System Applicable for Humid and Windy Areas, Working with Various Nanofluids. *Journal of Cleaner Production*, **296**, Article 126579. https://doi.org/10.1016/j.jclepro.2021.126579

[28] Novaes Menezes, E.J., Araújo, A.M. and Bouchonneau da Silva, N.S. (2018) A Review on Wind Turbine Control and Its Associated Methods. *Journal of Cleaner Production*, **174**, 945-953. https://doi.org/10.1016/j.jclepro.2017.10.297

[29] Arslan, T., Bulut, Y.M. and Altın Yavuz, A. (2014) Comparative Study of Numerical Methods for Determining Weibull Parameters for Wind Energy Potential. *Renewable and Sustainable Energy Reviews*, **40**, 820-825. https://doi.org/10.1016/j.rser.2014.08.009

[30] Medjo Nouadje, B.A., Kelly, E., Tonsie Djiela, R.H., Tiam Kapen, P., Tchuen, G. and Tchinda, R. (2024) Chad's Wind Energy Potential: An Assessment of Weibull Parameters Using Thirteen Numerical Methods for a Sustainable Development. *International Journal of Ambient Energy*, **45**, Article 2276119.

https://doi.org/10.1080/01430750.2023.2276119

[31] Mirhosseini, M., Sharifi, F. and Sedaghat, A. (2011) Assessing the Wind Energy Potential Locations in Province of Semnan in Iran. *Renewable and Sustainable Energy Reviews*, **15**, 449-459. https://doi.org/10.1016/j.rser.2010.09.029

[32] Bataineh, K.M. and Dalalah, D. (2013) Assessment of Wind Energy Potential for Selected Areas in Jordan. *Renewable Energy*, **59**, 75-81. https://doi.org/10.1016/j.renene.2013.03.034

[33] Oyedepo, S.O., Adaramola, M.S. and Paul, S.S. (2012) Analysis of Wind Speed Data and Wind Energy Potential in Three Selected Locations in South-East Nigeria. *International Journal of Energy and Environmental Engineering*, **3**, 1-11. https://doi.org/10.1186/2251-6832-3-7

[34] Al-Addous, M., Al Hmidan, S., Jaradat, M., Alasis, E. and Barbana, N. (2020) Potential and Feasibility Study of Hybrid Wind-Hydroelectric Power System with Water-Pumping Storage: Jordan as a Case Study. *Applied Sciences*, **10**, Article 3332. https://doi.org/10.3390/app10093332

[35] Fagbenle, R.O., Katende, J., Ajayi, O.O. and Okeniyi, J.O. (2011) Assessment of Wind Energy Potential of Two Sites in North-East, Nigeria. *Renewable Energy*, **36**, 1277-1283. https://doi.org/10.1016/j.renene.2010.10.003

[36] Poompavai, T. and Kowsalya, M. (2019) Control and Energy Management Strategies Applied for Solar Photovoltaic and Wind Energy Fed Water Pumping System: A Review. *Renewable and Sustainable Energy Reviews*, **107**, 108-122. https://doi.org/10.1016/j.rser.2019.02.023

[37] Kidmo, D.K., Bogno, B., Deli, K. and Aillerie, M. (2021) Assessment of the Rural Water Supply Potential by Mechanical Wind Pumping around the Floodplains of Lake Chad. *Energy Engineering*, **118**, 931-945. https://doi.org/10.32604/ee.2021.015574

[38] Abbas, M., Belgroun, Z., Aburidah, H. and Merzouk, N.K. (2013) Assessment of a Solar Parabolic Trough Power Plant for Electricity Generation under Mediterranean and Arid Climate Conditions in Algeria. *Energy Procedia*, **42**, 93-102. https://doi.org/10.1016/j.egypro.2013.11.009

[39] Quan, P. and Leephakpreeda, T. (2015) Assessment of Wind Energy Potential for Selecting Wind Turbines: An Application to Thailand. *Sustainable Energy Technologies and Assessments*, **11**, 17-26. https://doi.org/10.1016/j.seta.2015.05.002